A Review on Surface Engineering Perspective of Metallic Implants for Orthopaedic Applications

SUDHAKAR C. JAMBAGI [1,3] and VINAYAK R. MALIK [2]

1.—Department of Mechanical Engineering, National Institute of Technology Karnataka, Surathkal, Mangaluru, Karnataka State 575025, India. 2.—Department of Mechanical Engineering, KLS Gogte Institute of Technology, Visvesvaraya Technological University, Belagavi, Karnataka, India. 3.—e-mail: sudhakar@nitk.edu.in

Orthopaedic metallic implant design is expected to meet two critical challenges—biocompatibility and mechanical strength. According to a survey conducted in 2017, the global market of implants will grow by ~46% by 2025. Researchers have been trying to alleviate the problems of these implants, namely, biocompatibility, microbial invasion, bio-inertness, corrosion, and wear. Surface modification techniques that operate at low temperature and diffusion-based processes are preferred to circumvent the problems. These methods include thermochemical (carburizing, nitriding, etc.), electrochemical processes (electrochemical deposition, chrome plating, etc.), and ion implantation. This review presents the significance of these methods while meeting various challenges, such as wear, biocompatibility, and corrosion. The implants reviewed are stainless steel, Co-Cr alloys, titanium alloys, and magnesium alloys. Finally, the friction-stir process, another low-temperature process, has been reviewed for Mg and its alloys.

INTRODUCTION

Physiological functions of damaged biostructure can be restored through appropriate bio-implants, and the demand for such implants is expected to grow substantially. The size of the orthopaedic implants market was estimated at US$45,901 million in 2017 and is expected to reach $66,636 million by 2025, increasing at a compound annual growth rate of 4.7% between 2018 and 2025.

Typical applications of metallic implants include replacing joints (e.g., knee, hip, and shoulder prosthetics), and screws and plates for fixation of bones and dental implants. The following metallic implants have been extensively used: SS (316L SS and 316L VM), Co-Cr alloys (Co-Cr, Co-Cr-Mo and Co-Ni-Cr-Mo), and titanium and its alloys (Ti-6Al-4V, Ti-Nb-7A-Zr, Ti-Ni-Ta, Ti-Sn-Nb and Ti-15MO-5Zr-3A). Although metallic implants possess superior mechanical properties, they lack corrosion resistance and deteriorate when the ion concentration increases, eventually entailing routine surgery.

Therefore, there is a great need to tailor the surface chemistry to tackle corrosion without losing biocompatibility, avoiding microbial invasion. Figure 1 shows the statistics of the published literature in this context.

METALLIC IMPLANTS: MATERIALS, PROCESSES, AND CHARACTERISTICS

Stainless Steel (SS)

Bio-implants made from 316L SS and 316L VM are widely used in this category. However, SS shows pitting and crevice corrosion when exposed to chloride ions present in the blood. Initial research also showed a close correlation between corrosion pits and ions in SS.[1,2] Amel-Farzad et al.[3] examined a femoral implant, which had fractured in patients' thighs during its service, and the failure was attributed to corrosion fatigue assisted by crevice corrosion.[3] On the other hand, metal ions liberated during use might lead to local inflammation and subsequent loosening of replaced joints. These ions were liberated when body fluids reacted with oxygenated saline solution at pH 7.4 (37 °C).[4] Of many constituents, Ni has been found to be the most
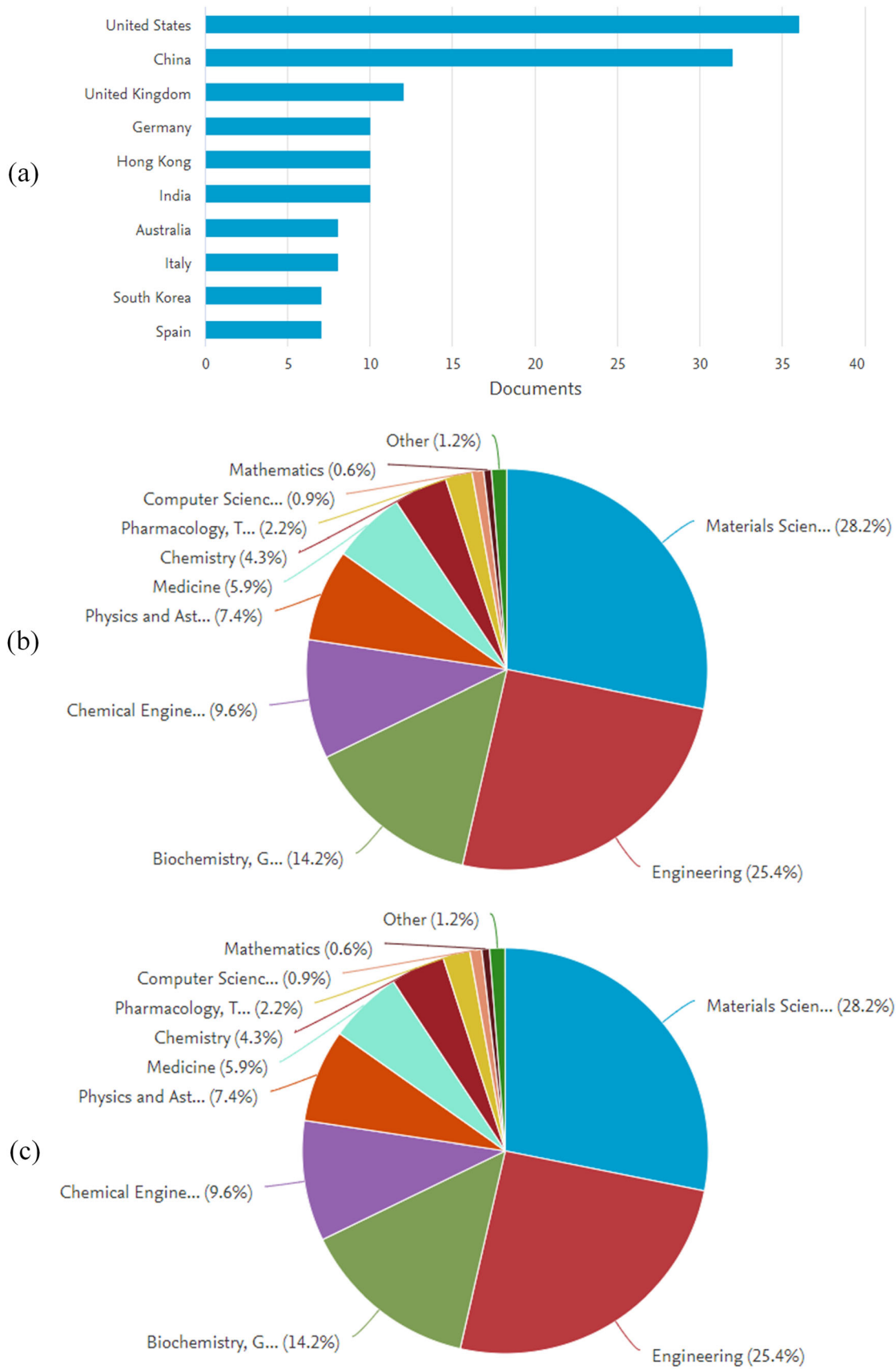
Fig. 1. Search results from Scopus on surface engineering/modifications of metallic orthopaedic implants. Number of documents published from 1984 to 2020: (a) by country (sequenced in ascending order for the top 10 countries), (b) by subject area, and (c) type of articles.

toxic.[5] Furthermore, the difference between the elastic modulus of SS ($\approx$ 200 GPa) and natural bone (3–20 GPa) results in joint separation over a period. However, SS would be preferable for temporary fracture fixation devices due to its cost-effectiveness.[6,7]

For 20 years of duration, the implant may undergo $\sim 1 \times 10^7$ cycles of loading, and the implant may fail well below its yield strength or tensile strength.[8–10] Also, SS implants suffer from poor wear performance, and the debris causes an allergic reaction when it comes in contact with surrounding tissues.[11]

Titanium and its Alloys

In metals, titanium is the widely used material for bio-implants for biocompatibility and low density associated with higher corrosion resistance.[12–14] Another advantage of Ti is its non-toxicity, as excess titanium is excreted with no digestion or absorption in the human body.[15] Among various Ti alloys, Ti-6Al-4V containing lower oxygen and iron concentrations has dominated the commercial market. The corrosion resistance of Ti-6Al-4V can be further enhanced by the addition of Nb, due to the formation of a tenacious oxide layer. However, the stability of these oxide layers dictates the longevity of the implants. Upon abrasion, the implant generates particulate debris causing a harmful effect over the long term. Further, ill-effects of Al and V in Ti-6Al-4V have been reported, which manifested in the form of peripheral neuropathy and osteomalacia.[16,17] Efforts are being made to develop β-titanium alloys with a lower modulus of elasticity to minimize the stress shielding effect.[18,19]

Cobalt-Chromium Alloys

The desirable wear resistance makes these alloys attractive in orthopaedic applications, like complete joint replacement for hip and knee regions. However, they come with a limited ductility of $\sim$8%. However, this offers better resistance to corrosion in the chloride environment due to the formation of the Cr_2O_2 passive oxide layer. Co-Cr, Co-Cr-Mo, and Co-Ni-Cr-Mo are a few of the alloys used. The major drawbacks of these alloys are allergy and carcinogenicity. Paustenbach et al.[20] reported that an increased cobalt concentration in the blood could result in cardiovascular, endocrine, hematological, and neurological disorders. This concentration was limited to 300 μg/L. The modulus of elasticity of Co-based alloys is 230 GPa which is 10 times that of cortical bones in humans.[21] This difference might lead to a stress shielding effect preventing stress transfer to nearby bones and might become a cause for bone atrophy (reduction in density).[22]

The implants mentioned above are permanent ones. Recently, temporary implants have been introduced to heal the tissue and metabolize it in the human body without leaving any residues.

Magnesium and its Alloys

Mg alloys are the most common degradable implants. They tend to oxidize in the presence of water, releasing H_2 gas, and this degradation causes a pitting corrosion. However, the corrosion rate accelerates in the presence of impurities like nickel, copper, and iron, a phenomenon which occurs primarily when Fe, Ni, and Cu compounds are > 0.005 wt% in the implant. Qiao et al.[23] noticed a drastic increase (3–60 times) in the corrosion rate of pure Mg with the increase in Fe content (26–48 ppm). Immersion tests with aqueous 3.5% NaCl were used to characterize the corrosion behavior. Similar results were observed by Song [1] in pure Mg in Hank's solution. The yield strength of Mg implants relies on their manufacturing history: for example, 21 MPa by casting, and, for as-cast Mg, 90–105 MPa by extrusions and 115–140 MPa by rolling.[24] Hence, researchers are striving to improve the mechanical properties by adding less toxic alloying elements. These elements are Ca, Sr, Zn, Si, Sn, Zr, Al, and rare earths.[25] Nonetheless, achieving good mechanical strength and corrosion resistance has been a significant challenge. Attempts have been made through processing techniques; for example, Pu et al.[26] and Etim et al.[27] reported improved corrosion resistance by deformation processing, which was attributed to grain size reduction and the dominant basal-textured orientation of the grains.

Iron and its Alloys

Fe-based degradable biomaterials are a potential substitute for Mg alloys due to their superior mechanical properties, comparable with SS. The major drawback is their slow degradation rate in body fluids, and the traces left often contaminate blood. Moreover, their magnetic susceptibility interferes during magnetic resonance imaging (MRI) scans of the implanted patient. Hence, research has been focused on enhancing the degradation rate and improving MRI compatibility.[28] The significant grain boundaries often promote corrosion, which is curbed by increasing the grain size. Therefore, electroformed Fe performs better as compared to cast Fe.[29] Traces of Mn and Pd can enhance the mechanical strength and act as cathodic sites, further accelerating biodegradation.[30] Furthermore, increasing the Mn content ($\approx$ 30 wt%) introduces anti-ferromagnetic qualities in Fe.[31,32] Moreover, friction-stirring bulk implant material

results in grain refinement with a higher count of high-angle grain boundaries.[33]

In temporary implants, Mg, Fe, and Zn alloys.[34] have been most widely used because of their in vivo biocompatibility, controlled degradation rate, sufficient strength to support bone tissue, and help in bone growth. Mg and its alloys closely resemble the natural human bone, and hence they have been reviewed.[35]

The issues encountered by the metallic implants, in either in vivo or in vitro conditions, are highlighted through Fig. 2.

SURFACE PREPARATION

Both roughness and wettability of the implant significantly influence its biocompatibility. However, a rough surface is more susceptible to bacterial adhesion.[36] SS surfaces have been polished using electropolishing with or without acid etching.[36] Sometimes, electropolishing may be insufficient for cell adhesion. Hence, the surface contact angle can be further decreased using chemicals, such as HNO_3 + HCl, with which the roughness $\sim Ra \leq 10$ nm could be achieved. The electropolishing process is by micro-polishing which allows controlled anodic dissolution of the rough surface under the influence of an electric charge.[36–38] Latifi et al.[38] first used this process and studied the roughness and cell viability (survival of cells) inter-relationship,[38] and it was proved that nanoscale roughness is sufficient for initial protein adhesion as well as cell adhesion and proliferation.[39] This technique eliminates the surface contaminants and oxides essential in regulating intactness between bone tissue and the implant surface. For SS, electropolishing and electrodeposition techniques are economical compared to the processes demanding sophisticated instrumentation: plasma-assisted chemical vapour deposition or laser treatment.[38,40] Most recent work by Mas Ayu et al.[41] has studied the cell adhesion cell growth of biological grade Co-Cr-Mo alloy etched by

mechanical (Ra-0.1 $\pm$ 0.02 μm) and chemical(1.63 $\pm$ 0.15 μm) means. The resulting microstructure showed pores with large surface areas, which is a desirable feature for cell adsorption and growth.

Surface Modification Techniques

The metallic implant properties can be improved by processing methods, alloying, and surface modification techniques. The implants should possess (1) biocompatibility, (2) sound mechanical properties, and (3) corrosion resistance.[5,11,42,43]

Two methods can effectively tailor the implants' properties: (1) by alloying the metal implants to suit the functionality, and (2) by modifying the surface chemistry of the implant.[44] The former has had some adversaries. For example, the release of aluminum and V_2O_5 into the body can cause serious illnesses, such as peripheral neuropathy, osteomalacia, and Alzheimer's disease. Consequently, surface modification has been the preferred choice.[45,46]

However, the processing temperature directly influences the biocompatibility of implants. Large thermal gradients induce inhomogeneity in the microstructure, leading to the formation of detrimental phases in it. For instance, in the Ti-6Al-4V alloy, during selective laser melting, the following undesirable changes occur: (1) segregation of the aluminum, (2) precipitation of the Ti_3Al intermetallic phase, and (3) the formation of elongated grains.[47] An inert atmosphere can circumvent oxidation. Further, low-processing temperatures are suitable for handling thermolabile materials and temperature-sensitive additives/reinforcements and avoiding loss of bulk properties. Hence, this review advocates low-temperature surface modification techniques.

In the ASM handbook, surface engineering is defined as the process of tailoring the surface and subsurface properties of the implant to augment its properties to meet the intended function.[48]
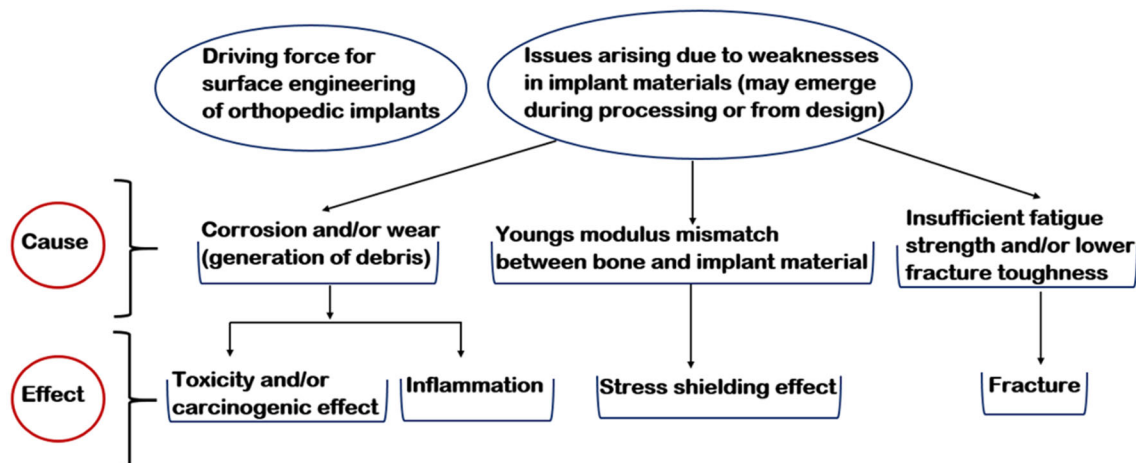

Fig. 2. The relationship between cause and effect of failure in orthopaedic metallic implants.

Surface modification can be broadly classified into the following two categories:[49–51]

1. A new material is deposited onto the surface as a coating.

2. A technology that changes the surface chemistry dealing with the diffusion of the elements.

The thermal spray process uses a heat source to melt and deposit the molten particles onto a substrate. The most common thermal spray processes include plasma spray, flame spray, etc.[51] These processes suffer from several drawbacks: (1) the heterogeneous microstructure of the coatings, (2) poor crystallinity, which may lead to bone resorption, and slackness in the implants, (3) thick coatings lacking homogeneity delaminate quickly, and (4) residual stress has been the primary concern.[52,53]

However, surface modification is economical and promising for metallic implants to achieve the desired mechanical properties, corrosion and wear resistance, and biocompatibility.[46,54–56] The processes used for this purpose are thermochemical diffusion techniques (carburizing, nitriding, boronizing; Fig. 3), and electrochemical processes (electrochemical plating, chrome plating, and phosphating), and ion implantation. These processes promise to impart superior mechanical strength and biocompatibility.

Low-temperature (< 1000 °C), diffusion-based surface modification techniques offer the following advantages;[46,54–57]

(i) The coatings are economical, reliable, and high quality.

(ii) A coating/substrate with homogeneous microstructure

(iii) Coatings endow high hardness, wear resistance, and corrosion resistance.

(iv) Biocompatibility with osseointegration harnessing cell growth and proliferation.

Thermochemical processes

Non-metal or metal atoms are diffused onto the surface of the base metal. The standard thermochemical processes are listed below.

Carburizing

A surface hardening to produce a carbon-rich surface by the diffusion process. Thermal carburization is the process that uses either a gas or laser source, and, for gas carburizing, the gaseous mixture of propane and butane.[55] The typical temperature range is $\sim$850–950 °C, and the carbon content ranges from 0.2 to 0.8 wt% (Fig. 3). Thus, a carburised sample produces hard compounds like TiC and V_4C_3 and reduces residual stresses,[49,50] and is carried out under vacuum to prevent oxidation. Carburizing induces surface roughness as low as Ra $\sim$0.04 μm, and is desirable for cell adhesion and cell proliferation.[58] Recently, a solid carburizing was introduced by Luo et al.[59] performed in a vacuum furnace with the carburizing media, $NaCO_3$, $CaCO_3$, and carbon powder. Thus, carburized $Ti_{13}Nb_{13}Zr$ alloys showed satisfactory results forming a TiC layer up to the thickness of 120 μm, and a hardness of the order of 812 HV was recorded at 1523 K against the untreated sample of $\sim$225 Hv. This improvement was attributed to the phase transformation from the hexagonal close-packed (HCP) phase to the β-phase of the body-centred cubic (BCC) crystal, and increased dislocation density, which helped achieve wear resistance and biocompatibility.

Nitriding (Fig. 3)

Thermo-diffusion process where nitrogen gas is incorporated onto the metal implant surface, wherein the thermal source could be flame, plasma, or laser.[60] For instance, a nitrided Ti-6Al-4V implant (at 850–900 °C) improved not only corrosion resistance and biocompatibility[60] but also hardness and wear resistance.[53]

Boronizing/Boriding

Here, boron elements are diffused at temperatures $\sim$840 1050 °C for 10 h duration (Fig. 3). This process is beneficial for achieving superior mechanical strength. For example, borided 316 L SS can produce hard components, like F_2B, Ni_3B, and CrB.[61]
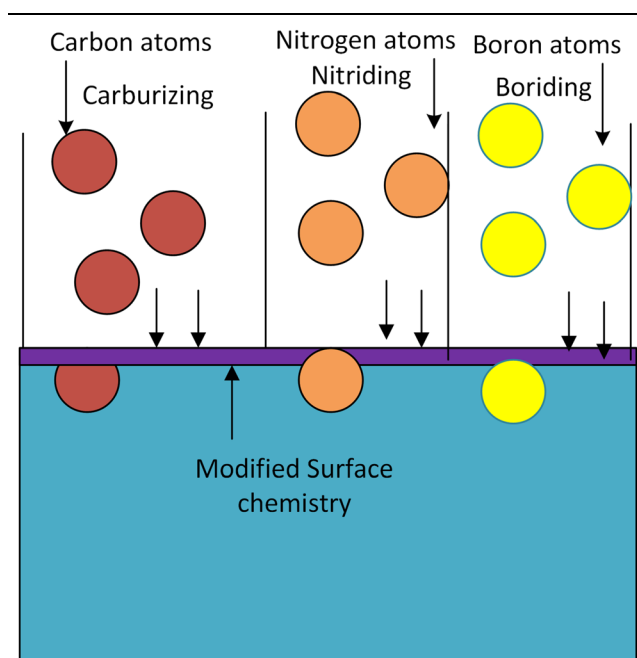

Fig. 3. Schematic to explain thermochemical diffusion processes: carburizing, nitriding, and boronizing.[50]

In addition, the other processes, such as electrochemical plating or electrodeposition, also seem to be more advantageous in converting bioinert material (SS) into bioactive by depositing a thin layer of bioactive material, hydroxyapatite (HAP), that eventually cultures living cells and multiplies them.[40]

Electrochemical Processes

Electrochemical Deposition

As stated earlier, high-temperature processes often exacerbate the crystallinity of phases, resulting in non-uniform coatings with microcracks,[63] consequently affecting the biocompatibility. Hence, a low-temperature, reliable, economical process such as electroplating is preferred over many surface engineering techniques. Figure 4 shows an Mg alloy, AZ31, being coated with HAP as electrolyte. On applying an electric potential, the HAP precursor migrates towards the cathode (substrate). The yellow gel tape can protect portions from the coating.[42,62]

Most recently, researchers have electrodeposited HAP coatings on Ti,[64] Co-Cr-Mo alloys,[43] and SS alloys[65] to gain corrosion resistance, biocompatibility, and osseointegration.[66]

Although chrome plating is known for its superior wear and high corrosion resistance, it seriously affects the biocompatibility. Afolaranmi et al.[67] studied the ill-effects of the release of chromium ions, which were DNA and chromosomal damage and other mental-related illness. Therefore, chrome plating is preferred for hard structural applications.

Phosphating

Implants are treated with a dilute solution of phosphoric (H_3PO_4) at a temperature of $\sim$60–65 °C to improve their corrosion resistance. Xu et al.[68] reported improved corrosion resistance of Mg-Mn-Zn alloy which was evaluated by an electrochemical test set at 37 °C in 0.9% NaCl solution.
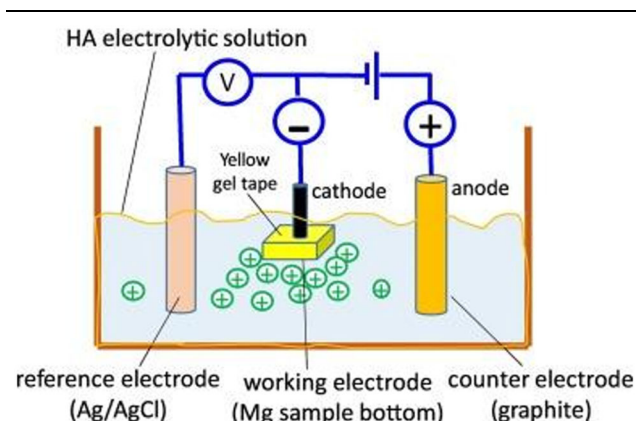
Potentiodynamic polarization (PDP) curves showed higher corrosion resistance and lowered current density compared to untreated samples. This improvement was attributed to the formation of a stable passive layer called brushite (CaHPO$_4$.2H$_2$O). However, this layer dissolves in HAP when it comes in contact with simulated body fluid (SBF) solution. Recently, Zhang[69] showed improvements in the in vivo and in vitro performance of Mg alloys with reduced pitting corrosion.

Ion-Implantation

An alloy up to a depth of $\sim$1 μm can be formed when high energy ions, typically of the order of 20–200 KeV, are impinged on the substrate surface, creating an ion-implanted surface (under vacuum) (Fig. 5).[71] The process involves two steps.[72] First, accelerated ions are formed from the atom, then, they are steered through a set of magnetic lenses to the target.[73] This process was carried out to enhance the corrosion and wear resistance of Ti and the biocompatibility of SS. At least $\sim$1 to $3 \times 10^{17}/cm^2$ C ions are required to combat corrosion, and more than $4 \times 10^{17}/cm^2$ ions for the wear-resistant layer.[55] With this, the pitting and crevice corrosion of SS can be largely controlled. In addition, HAP can be ion-impregnated onto the SS to enhance its biocompatibility.[39,57]

Various types of ions can be diffused into the metal to improve the properties: C^+ and Co^+ ions implanted achieve better osseointegration and corrosion resistance; similarly, Ca and P ions for biocompatibility; also, O and N for corrosion and wear resistance;[57] and F ions for crystallinity of phases.[39] Thus, ion implantation operates at a low temperature and offers flexibility to tailor the properties of metallic implants with ease in both in vitro and in vivo conditions. Another variant that operates at low temperature, plasma-immersion ion

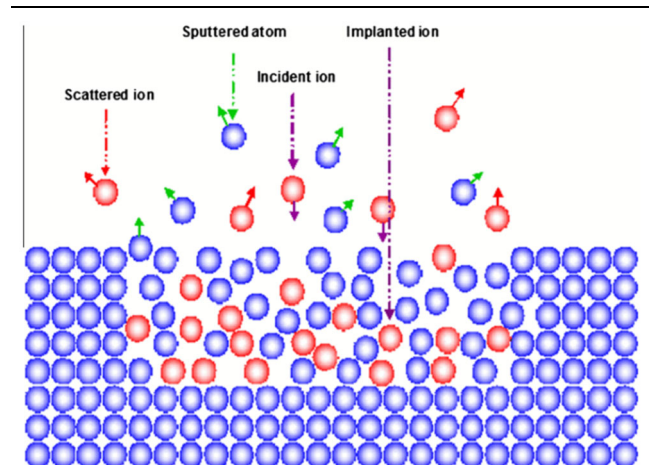Fig. 4. Schematic of electrodeposition technique. Reprinted with permission from Ref. 62.

Fig. 5. Schematic of ion implantation. Reprinted with permission from Ref. 70.

implantation (PI3), is gaining attention for its speed
and cost-effectiveness.

Friction-Stir Process (FSP)

FSP is a severe plastic deformation process
deforming the material primarily under shear conditions. A non-consumable tool rotating at high
speed plunges into the intended work material,
dwells, and traverses at the predefined speed.[74] The
microstructure primarily depends on temperature,
strain, and strain rates (Fig. 6).

This process can ease the higher-temperature
ailments of implants with better metallurgical
benefits. The most influencing parameters are tool
rotation speed, traverse speed, tool tilt angle, axial
force, and tool geometry. However, tool geometry
plays a significant role in achieving microstructural
homogeneity, the degree of material mixing if
alloyed/reinforced.[75,76] Efforts have been made to
fabricate surface composite layers with particulate
reinforcements incompatible with the implant at
elevated temperatures,[77] in order to achieve a
unique combination of mechanical and tribological
properties.[78]

Metallic materials, such as stainless steels, titanium and its alloys, and cobalt alloys, are commonly
used as orthopedic implants due to their excellent
strength and toughness; however, they suffer from
poor corrosion, biocompatibility, and wear resistance. The following section discusses low-temperature surface-engineered metallic implants'
biocompatibility, corrosion, and wear properties.

STAINLESS STEEL (SS)

The effect of carburizing, nitriding, and ion
implantation on the cytocompatibility of austenitic
316L SS was first studied by Bordjih et al.[58] Carbon
was doped on the SS surface using reactive magnetron sputtering (at 200 °C), Plasma nitriding was
carried out below 400 °C, and nitrogen ion implantation was carried out using glow discharge without
mass separation energy ranging from 30 to 60 keV.
All the samples showed improvements in the hardness of the samples owing to the diffusion of C and
N atoms. The cytocompatibility of the samples was
assayed using fibroblast and osteoblast cells.
Around 3×10^3 cells per cm^2 were seeded onto the
sample and cultured at 37 °C for 21 days.

The cell viability results are shown in Fig. 7.
Plasma nitriding of SS failed to hinder the cell
growth due to toxicity. However, the study did not
consider the nitrogen concentration and its temperature variation. These aspects could have limited
the failure in cytocompatibility. The cell viability
was examined for 21 days. A wear test was conducted using a pin-on-disc (POD) test rig with
Hank's balanced salt solution (HBSS) as a lubricant. The corrosion resistance of samples was
investigated using a cyclic potentiodynamic test
performed in HBSS as an electrolyte. A fixed area of
0.8 cm^2 was exposed in each experiment and the
scanning rate was fixed at 1 mV/s. The current
densities for untreated, nitrided, carburised, and N-
implanted SS were 12.6, 6.9, 0.6, and 0.9 $\mu A/cm^2$,
respectively. Furthermore, the microstructure analysis revealed the decrease in cell density for the
nitride samples due to disruption in the protein
metabolism rate. Cell viability could have been
achieved through proper optimized parameters during nitriding. Therefore, low-temperature, diffusion-based surface-modification processes were
quite effective in controlling corrosion and the
longevity of the biocompatible implant.

For SS implants, osseointegration has been a
significant concern. This limitation has been alleviated by depositing bioactive HAP ($Ca_{10}(PO_4)_6(OH)_2$)
coatings on the metallic implants.[40,79] There are
quite a few techniques to deposit HAP onto a SS
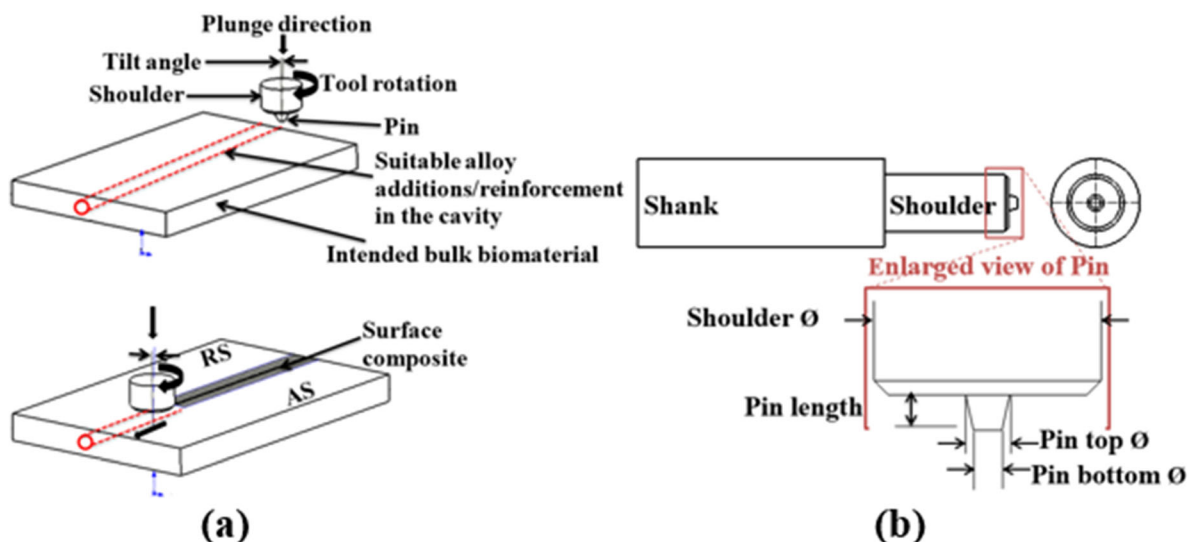substrate. Among them, electrochemical deposition

Fig. 6. (a) Schematic of FS process layout just before the plunge phase during the traverse phase, and (b) the tool.
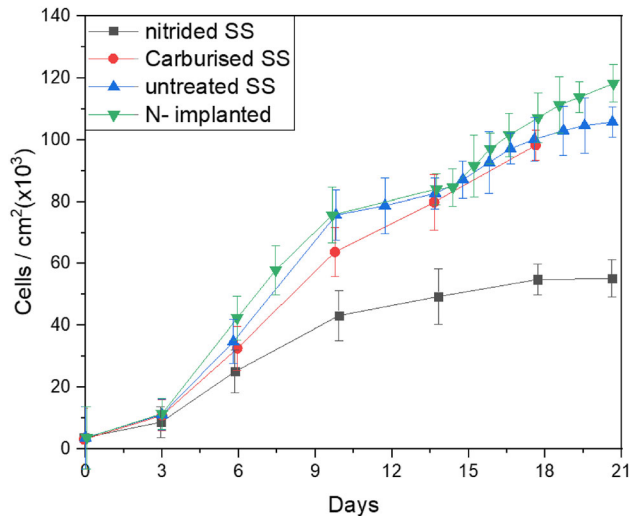
Fig. 7. Osteoblast cell viability for untreated, carburized, nitrided, and N-implanted austenitic stainless steel.[58]

promises to offer a uniform coating with improved hardness and resistance to cytotoxicity.[36] Recently, Pham et al.[65] performed an in vivo analysis of electrodeposited nano-HAP/SS implants when implanted in dog femur. The coating was deposited at a temperature in the range of 25–60 °C. The diffused atoms with the temperature rise helped develop the microstructure, cell adhesion, and proliferation. Optical microscope images revealed signs of osteoblast activity but no indication of osteitis.

Similarly, Thanh et al.[80] reported in vitro biocompatibility of electrochemically deposited HAP/316L SS implants in the presence of SBF solution. The potentiodynamic results were inconsistent, and the dissolution of the implant was observed after 7 days. This degradation was attributed to the loss of crystallinity. However, after 17 days, the pristine HAP started precipitating on the implant. Such behavior of implants is expected in in vivo conditions of tests that manifest their bio-activeness. The 316L SS implant is not susceptible to intergranular corrosion due to its low carbon content, and is protected against corrosion by a spontaneously formed iron oxide layer. This layer enhances corrosion resistance, inertness in biological fluids, passivation, improved wear, and adhesion characteristics. During electropolishing of SS, a dark iron oxy-hydroxide was observed, which acts as a passive layer against corrosion. Subsequent etching in HF acid showed traces of chromium oxide, which further fortified the passivation and hence corrosion resistance.[38,81]

Most recently, Samanta et al.[56] investigated wear resistance for a SS implant, which was plasmanitrided and subsequently coated by multilayer Ti/TiN. Coatings of eight layers of TiN were deposited on the Ti implant by using a direct current reactive magnetron sputtering chamber. The TiN coatings were uniform and less porous with columnar grains. However, the nitride samples were thinner in

comparison, showing the presence of compressive stresses. Wear resistances were compared for SS, SS with multi-layered Ti/TiN coatings, and SS sandwiched plasma nitride (PN) multilayer coatings, which showed good adhesion strength. These components performed better in wear resistance tests as analyzed by the hip simulator software against ultrahigh molecular weight polyethylene acetabular cups. This improvement was attributed to the high adhesion strength, hardness, and fracture toughness of duplex coatings. The multi-layered TiN coatings exhibited poor wear performance, as their adhesion was poor. The abrasion and fatigue wear mechanisms were predominant. However, the in vivo results were not reported.

Therefore, the surface modification techniques have still not lost their credibility in enhancing the properties like wear by forming carbides and reducing the coefficient of friction (COF). Most recently, Hammood et al.[82] have reported an improved corrosion resistance when a composite HAP/TiO2 was electrodeposited (voltage 20–40 V) onto a duplex SS substrate. Duplex SS substrates with an equal amount of ferrite and austenite can improve mechanical properties and corrosion resistance. However, the samples deposited above 30 V showed good resistance to corrosion, as identified by the potentiodynamic curves because their microstructure was uniform and dense.

Co-Cr Alloys

Co and Cr ion release has been a significant problem in these types of permanent implants. The PI3 process was used by in the temperature range of 300–350 °C to diffuse nitrogen and oxygen ions to control ion release. The corrosion study was performed in bovine serum, and the PDP curves were analyzed. Corrosion testing was performed in the presence of bovine serum at 37 °C. A conventional three-electrode cell had a Pt wire as counter electrode, an Ag/AgCl as reference electrode, and an ion implanted sample as a working electrode. An area of 0.125 cm^2 was exposed for 1 h with a potential sweep rate of 0.17 mV/s. Nitrogen-implanted samples performed poorly on the corrosion front as compared to oxygen-implanted samples. This result implied Co-Cr ion release, and nitrogen implantation failed to stop this migration from the implant. However, the oxygen at the temperature of 300–350 °C could effectively produce stable passive Cr_2O_3 and protect the surface from pitting corrosion.

The CoCr alloys are susceptible to corrosion. Cassar et al.[84] studied the corrosion behavior of a carburized CoCr alloy. The heat treatment was performed below 500 °C. Electrochemical impedance spectroscopy inspection was performed on the sample in the presence of Ringer's solution with a pH of 7.4. A stable, thick (i.e., low-capacitance) passive film of a carbon-rich solid solution called the

S phase or the expanded austenite phase was found on the surface. Because of this layer, the treated sample showed lower polarising resistance, i.e., higher corrosion resistance, than the untreated sample. However, during the last 4 h of testing, the corrosion resistance dropped for both samples. This phenomenon was left unexplored, and the physical implant was not subjected to any post facto inspection.

Titanium Alloys

The biocompatibility of titanium and its alloys has been a serious concern because of corrosion. Czarnowska et al.[85] investigated the in vitro analysis of a titanium alloy (OT4-0) subjected to nitriding and oxidizing. The nitriding was performed at 850 °C for 4 h and the oxidation at 400 °C for 2 h. The nitride sample was harder (1950 Hv0.05) than the oxidized sample (500 HV 0.05). Anodic polarization curves were measured in 0.5 M NaCl aqueous solution. The oxidized samples displayed high stability in corrosion resistance due to a TiO_2 passive layer, as observed by the PDP curves. In vitro biocompatibility studied with human fibroblast cells showed good cell adhesion and no signs of cytotoxicity. In another report, Zhang et al.[86] used double glow discharge plasma hydrogen-free carburizing for the Ti6Al4V alloy to study the implications on hardness and corrosion resistance. The microstructure showed that the thickness of alloyed layer was 100 μm in the presence of TiC, C, and TiAl3 phases. Due to the presence of TiC, the alloy's hardness was improved, and PDP, in the presence of 5% H_2SO_4, showed an improvement in corrosion resistance which was attributed to the depletion of V and Al compounds at the onset of the carburization process.

Luo et al.[59] investigated the tribological properties of solid carburized $Ti_{13}Nb_{13}Zr$ alloy. The carburization was performed at different temperatures for 2 h in a vacuum furnace. A hardness of 812 HV was recorded corresponding to the temperature of 1523 K against the untreated sample hardness of ~203 Hv. The microstructure showed a 125-μm-thick carburized layer. The better hardness was attributed to the formation of TiC. During this process, the α-phase having a HCP phase transformed to the β-phase of the BCC crystal. In other words, an untreated sample having $\alpha + \beta$ was transformed to β. The rise in dislocation density was another reason for the increase in hardness. Finally, ball-on-plate configuration was used for the wear test. The test parameters were an amplitude of 3.5 mm, a normal load of 30 N, and z sliding frequency of 1 Hz. The tribotest was conducted both in the dry and in the presence of serum lubrication. Under lubrication, the coefficient of friction was reduced to 0.16 ± 0.03 against the dry tested sample of 0.37 ± 0.06. Because of this low COF, corresponding to a carburizing temperature of 1473 K, the wear rate was reduced to 0.661×10^{-9} kg/N-m from

1.735×10^{-9} kg/N-m. This improvement was attributed to the formation of a hard TiC phase.

Mg Alloys

Although Mg and Mg alloys possess good mechanical properties, pitting corrosion has been inevitable due to H_2 gas evolution for such implants. Because of this limitation, the biocompatibility of such implants is affected. Virtanen[87] reviewed the biocompatibility and corrosion resistance of various Mg and Mg alloys. Pure Mg is susceptible to corrosion due to its high electrochemical potential (− 2.3 V).[44,88] The report explains the primary mechanism of pitting corrosion, a severe degradation phenomenon. The pH shift was an apparent reason during H_2 gas evolution, and was regarded as a boon for some cases and a bane in others, as being concerned with the passivation of the $Mg(OH)_2$ layer.[88,89] However, according to Agarwal et al.,[88] the presence of $HPO_4{}^{2-}/PO_4{}^{2-}$ and $HCO_3{}^-/CO_3{}^{2-}$ anions and Ca^{2+} ions, forming calcium phosphate and carbonate salt precipitates, protect the erosion of the passivation layer on Mg and its alloys, thereby preventing the possibility of pitting corrosion.[44]

Song et al.[90] compared the corrosion resistance of three electrodeposited Ca-P coatings on a biodegradable Mg-Zn alloy. The three layers were brushite, HAP, and fluoridated HAP (FHA). Of these, the FHA coatings outperformed the other two coatings. The FHA coating was bioactive and offered nucleating sites for apatite formation, and the coating was stable and corrosion-resistant. Although implants displayed good corrosion resistance and bio-activity, the detailed in vivo and in vitro characterizations of the implants were missing in this report. Similarly, when pure Mg alloyed with Ca, the secondary phase Mg_2Ca improved the mechanical and corrosion resistance. The Ca refines the grain,[91,92] and Zn acts as a good solid solution and precipitation strengthening agent.[91,93]

FSP is another processing technique that uses frictional heat to homogenize the mixture of materials at the interface of the metallic implant. The following sections review the corrosion aspects of Mg and its alloys consolidated through the FSP route. Kannan et al.[92] reported on the in vitro analysis of friction-stir-processed (FSPed) AZ31 alloy. The study showed an improvement in corrosion resistance which was attributed to the homogenous dispersion of the alloying elements, such as aluminum, calcium, and rare earths, in the alloy and the precipitation of the secondary phase of $Mg_{17}Al_{12}$.[92,93]

Further, the effect of grain refinement during FSP on the bioactivity of magnesium implants was reported by Ratna Sunil et al.[94] The FSP tool had a tapered pin made of H-13 tool steel. A rotational speed of 1200 rpm, a load of 5000 N, and a translational speed of 12 mm/min were selected.

The grain size decreased from 1500 μm to 6.2 μm in the nugget zone. The implant was immersed in SBF five timesfor 72 h to examine its bioactivity. The microstructure revealed magnesium hydroxide, HAP, and magnesium phosphate phases, which phases were responsible for controlled degradation. Furthermore, phosphorus-containing compounds, together with magnesium hydroxide, inhibit the aggressive action of chloride (Cl^-) ions. Eventually, the passive layer was protected. Moreover, the Ca/P ratio resists the aggressive action of the Cl^- ions.

Sodhi and Singh[89] attempted to develop corrosion-resistant Mg alloys by the FSP process. Microhardness and in vitro corrosion rates were determined. HAP was chosen as a reinforcement material for the pure magnesium alloy. A conical-shaped tool made from SS of grade 202 was used for FSP. The workpieces were FSPed using one pass under constant rotational (w), and traverse (v) speeds of 2000 rpm and 60 mm/min. The decrease in grain size from 820 to 150 μm was observed due to dynamic recrystallization (DRX). As a result, the microhardness has increased from 36 to 46 Hv. In conclusion, FSPed alloys showed improved corrosion resistance due to the phase changes and grain refinement. Recently, Durairaj[64] electrodeposited HA on AZ31 and Ti6AL4V alloys to study their relative performance in corrosion resistance and growth of the apatite layer in a body fluid. The PDP curves were analyzed for their corrosion resistance. The coated samples showed lower current densities than the uncoated samples. The SEM images showed a thick layer of apatite on both the coated samples after dissolving the samples in SBF for 7 days. The HA coating helped to reduce the corrosion rate to 1.477 mm/year and 0.062 mm/year for AZ31 and Ti6Al4V, respectively.

So far, the reviews have been confined to monolithic implants. Additionally, using reinforcements, such as Al2O3, SiC, and ZrO_2, can improve the corrosion resistance. Abbasi et al.[95] assessed the corrosion and wear performance of two FSPed AZ91 alloys reinforced with Al_2O_3 and SiC. The corrosion test was conducted in the presence of NaCl solution. The FSPed specimens showed an improvement in corrosion resistance, with lower current densities than the original alloy. This improvement was attributed to relief from residual stress due to the annealing effect caused by the stirring action during FSP. Later, Mazaheri et al.[96] investigated the corrosion performance of the FSPed AZ31/ZrO_2 alloy with one and four passes. The corrosion test was performed in 3.5 wt% NaCl aqueous solution. With four passes, the A31 alloy developed a passive film to protect against corrosion. With a single pass, the hardness improved by 65%, while, with four passes, the hardness doubled.

Zhao et al.[97] studied the corrosion resistance of nitrided Ti, SS316, and CoCrMo with and without surface modifications in phosphate buffer saline (PBS) solution maintained at pH 7.4 at room temperature. An Ag/AgCl/KClsat electrode was used as the reference electrode, and the counter electrode was a Pt wire. The testing sample (working electrode) was fixed at the bottom of the electrochemical cell, exposing an area of 0.78 cm^2 to the electrolyte. After the stabilization of the open circuit potential, the polarization curves were recorded dynamically using an Autolab PGSTAT 302 N Potentiostat at a scan rate of 0.8 mV/s in the cathodic to the anodic direction. The PDP curves for treated and untreated samples are shown in Fig. 8. Figure 8a shows the PDP curves for the Ti alloy. For a treated sample, an increase in anodic current with electrode potential indicates the release of metal ions without forming a passive layer. This phenomenon could be attributed to the higher temperature (740 °C) of the nitriding process. Figure 8b shows similar behavior for the SS sample, and a loss of passivation is observed at the electrode potential of 0 V. However, a stable passive layer is found to be still sustained for a sample nitrided at 400 °C. Figure 8c again illustrates the importance of a lower processing temperature, especially for such diffusion-based processes. Here again, the loss of passivation is observed for samples processed at 600 °C. At 400 °C, the passivation layer was consistent but with less stability, which could be attributed to the release of metal ions from the implant surface. In this case, Cr ions were ejected from the implant surface without forming a passive layer.

FSP has been the best choice for Mg alloys to attain superior mechanical properties and tribological properties. Asadi et al.[98] have investigated the effect of cooling and tool rotational direction on the microstructure and mechanical properties of FSPed AZ91. The FSP approach has been chosen as a solid-state process wherein the material is subjected to intense plastic deformation by a rotating tool. In this report, the FSP tool was a 2344 hot-working steel with a square pin. The rotational and traverse speeds were 900 rpm and 63 mm/min, respectively. FSP has enabled refinement of the microstructure from 150 to 4 μm and hence improved the mechanical properties. The microhardness has increased more than 75 HV for two passes regardless of rotation direction. FSP with two and four passes did not significantly affect the microstructure; however, there was significant improvement in microhardness with eight passes and a change in the rotational direction ($\sim$100 HV). The processed zone, called the stir-zone (SZ) comprises a fine equiaxed recrystallized grain structure obtained by DRX. Furthermore, changing the rotational direction caused a substantial decrease in the grain size of water-cooled samples.[98] The refined microstructure helped resist crack growth in the matrix during the tensile test, enhancing the elongation.[91] The tensile strength increased from $\sim$130 to $\sim$250 MPa. Subsequently, a wear test was performed using a POD test rig. The counter body was St52100 steel. A load of 50 N was applied with a slide speed of 1 mm/min
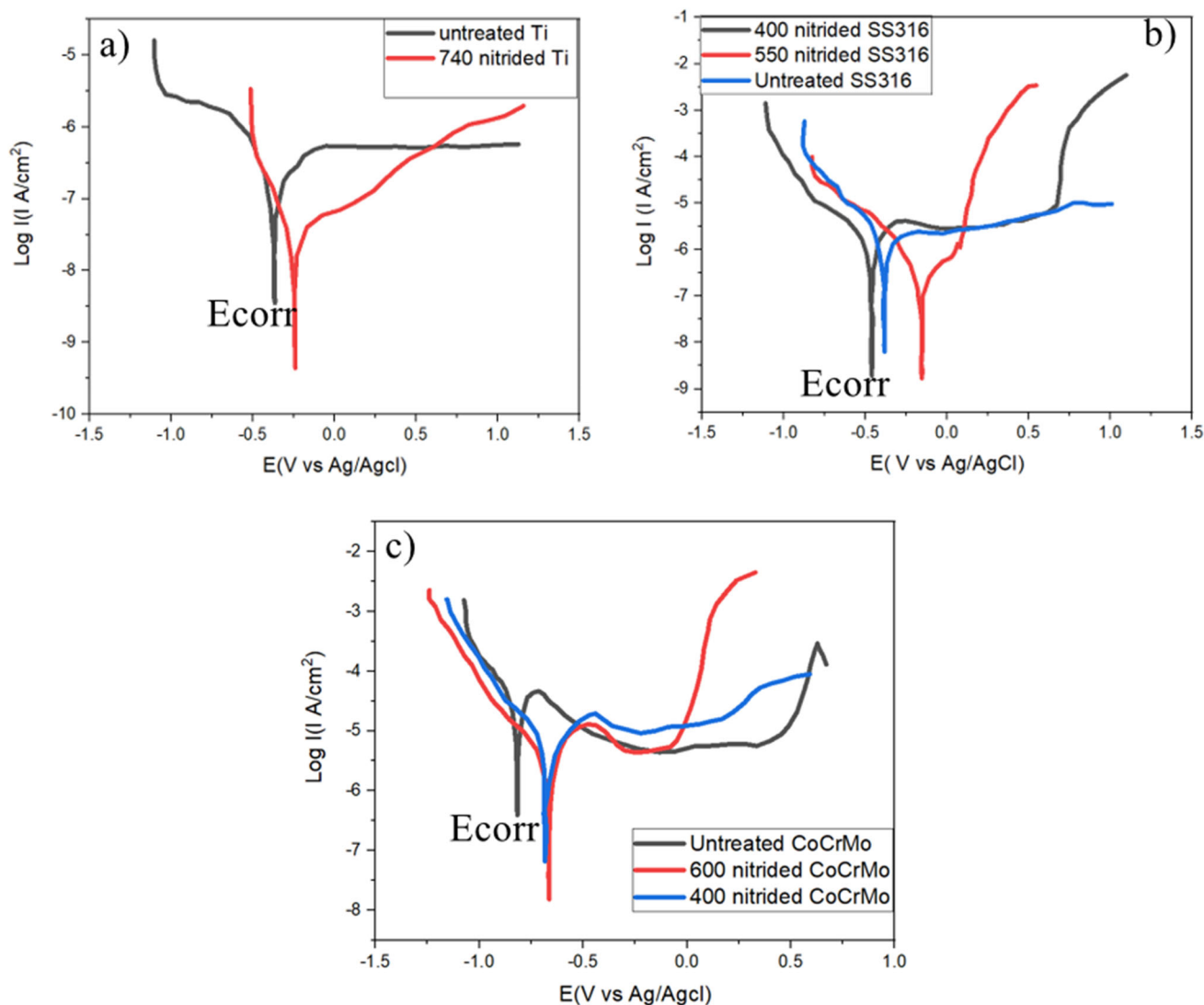
Fig. 8. Potentiodynamic polarization plots of potential versus log current density in PBS solution: (a) nitrided-Ti, (b) nitrided- SS316, and (c) nitrided CoCrMo. Reprinted with permission from Ref. 97

for a distance of 500 m. No significant wear improvement was found. An abrasive plowing mode of failure and micro-cutting mechanisms were observed in base metal and FSPed samples.

Madhusudhan Reddy et al.[99] reported on the wear resistance improvement of FSPed ZM 21 alloy reinforced with hard particles, such as SiC and B$_4$C particles. The grain-refined microstructure revealed homogenous dispersed carbide particles within the matrix phase. Before the wear test, an increase in hardness was reported and was attributed to the individual higher hardness of the carbide particles and the Orowan mechanism, where dislocation movements are hindered by carbide precipitates.[96] This phenomenon is also known as "grain pinning". A wear test was performed using a POD test rig, using hardened steel (65 HRC) as a counter body. FSP produced a lower coefficient of friction, and hard ceramic phases changed the wear mechanism from abrasive to adhesive.

Later, Abbasi et al.[95] assessed the corrosion and wear performance of two FSPed AZ91 Mg alloys reinforced with Al$_2$O$_3$ and SiC. The Mg alloy with carbide outperformed on both mechanical and corrosion characteristics. The FSP tool was cylindrical and was made of H13 tool steel. The FSP process was carried out in rotational (730–1800 rpm) and translational (14–80 mm/min) mode. The FSP tool was tilted by 2° from the workpiece's normal axis, and a mixture of dry ice and ethanol was applied as coolant. Additionally, different passes (one and four) were conducted to evaluate the effect of the number of passes on the properties of the specimens. It was observed that, by increasing the passes, the grain size was decreased, and the distribution of second-phase particles was improved; consequently, the hardness of the alloy was increased. The wear test was carried out using POD equipment with a SS 316 L (ASTM) disk as a counter face. The parameters for this test were a sliding speed of 1 mm/s, a normal

load of 50 N, and total sliding distance of 500 m. Although the hardness improved, this was not reflected in the wear performance. The predominant wear mechanism was adhesive. Kudła et al.[100] investigated the role of FSP on the microstructure and wear properties of the AM60 alloy. A cylindrical H13 tool steel was used. The presence of fine equiaxed grains was seen in the stirred zones. This improvement was attributed to an increase in the traverse speed compared to the rotational speed. As a result, there was an improvement in hardness and, hence, the alloy's abrasion wear resistance.

Similar improvements in wear resistance of FSPed ZK60 plates have been reported by Liu et al.[101] In this case, $MgZn_2$ precipitates were responsible for the improvements. The number of passes in FSP has been found to influence the wear performance, as observed by Mazaheri et al.[96] The tribological performance of the FSPed $AZ31/ZrO_2$ alloy was assessed for one and four passes. The FSP route could decrease $\sim$50% grain size of the ZrO_2-reinforced test coupon as compared to the plain AZ31 sample. Frictional heat and severe plastic deformation could not only eliminate deformed twins but also resulted in the formation of dynamically recrystalized grains. A wear test was performed on a reciprocating wear machine. The pin was made of AISI 52100 steel with a hardness of 63 HRC. The wear resistance of the reinforced alloy, processed with four passes, was better than the unreinforced counterpart with a $\sim$50 % drop in the COF. For the AZ31 alloy, the wear mechanism shifted from severe abrasion to adhesion, whereas with the ZrO_2 reinforcement, from severe abrasion to mild abrasion.

The effect of the tool pin profile on wear performance was studied by Vignesh Kumar et al.[102] A ZK60/SiC composite was FSPed using a tool made of M2 grade hardened to 65 HRC high-speed steel (HSS). The traverse speeds were set as 900 rpm and 10 mm/min, and tool tilt was 2°. During FSP, four different tool pin profiles were used, plain cylindrical, cylindrical thread, plain tapered cylindrical, and square. Of these, the tapered cylindrical pin exhibited superior properties attributed to the high shear force, homogeneous distribution of material, and balanced heat at the stir-zone, thus making it a defect-free zone. With the appropriate selection of tool, a $\sim$80% reduction in the average gain size was obtained which helped in the uniform dispersion of SiC particles, which are further responsible for grain boundary pinning. The grain refinement and dispersion strengthening enhanced the hardness to 121.2 HV0.5 from 66 HV0.5. A wear test was performed using the POD disc apparatus. The wear resistance was attributed to the higher hardness and well-dispersed SiC particles in the processed zone.

The literature shows that surface modifications are essential for metallic implants to control the dissolution rate in the presence of biological fluids.

Thus, in particular, low-temperature diffusion processes seem to be attractive alternatives in this domain. Furthermore, owing to their superior mechanical properties, multiwalled carbon nanotubes have also been selected as a reinforcement to improve the mechanical properties of HAP, which has been employed in many metallic implants for its bio-activeness.[53,103–105] However, these aspects are not discussed in this review paper.

Table I lists the selection of low-temperature, diffusion-based surface modification techniques to achieve biocompatibility, and corrosion and wear resistance of the metallic implants. From Table I, we can derive some conclusions, as follows:

(i)   The electrodeposition technique can be economically viable solution for all the materials.
(ii) A process like carburizing and nitriding could be the best choice for Ti alloys as they offer hardness to improve wear resistance.
(iii) The friction stir process could be beneficial for Mg and its alloys.
(iv) However, hybrid multi-layered coating processes can also offer better properties, but these processes are costly.

Thus, the low-temperature diffusion processes, carburizing and nitriding, were effective in improving the wear resistance by forming reacting phases. At the same time, FSP improves the mechanical strength by decreasing the grain size or forming hard phases within the microstructure. Such surface modifications are expected to impart much-needed longevity to orthopedic implants. Certain issues faced by metallic implants and the remedies suggested are listed in Table II.

Biocompatibility codes

Readers are also invited to refer to the latest standards recognized by the FDA*: ISO** 10993-1 Fifth edition 2018-08 (Evaluation and testing within a risk management process), ISO 10993-6 (tests for local effects after implantation), ISO 10993-11 (tests for systemic toxicity), ASTM F981-04 (for effect of Materials on Muscle and Bone), ASTM† F763-04 (for Short-Term Screening of Implant Materials), ASTM F1983-14 (Compatibility of Absorbable/Resorbable Biomaterials for Implant Applications).[107]

Future Scope

Austenitic SS is a feasible option even now due to its low cost and acceptable biocompatibility. The problem arises from constituents like Ni, which lead to the development of nickel-free high-nitrogen SS. Nitrogen acts as an austenite stabilizer and also helps in improving wear resistance. However, high

*FDA: Food and Drug Administration,

**ISO: International Organization for Standardization,

†ASTM: American Society for Testing of Materials.

Table I. Selection of surface modification techniques for different metallic implants to meet different challenges

Processes	Permanent implants			Temporary implants Mg and its alloys
	Stainless steel	Co-Cr alloys	Ti alloys	
Carburizing	B, W	C	B, C, W	–
Nitriding	W	–	B, C, W	–
Boriding	W	–	–	–
Electrodeposition	B, C, W	B, C	B, C	B, C
Phosphating	–	–	–	B, C
Ion implantation	B, C, W	C	–	–
FSP	–	–	–	B, C, W
Hybrid multilayer coatings	B, C, W	–	B, C, W	–

B Biocompatibility, *C* corrosion resistance, *W* wear resistance.

Table II. Metallic implants used in orthopedic applications and suggested surface modifications

Metallic materials	Problems encountered	Surface modification remedies [Ref.]	Major findings from the literature and remarks
Stainless steel	Poor wear, stress corrosion cracking	Duplex surface modification with plasma nitriding as mentioned in[56, 106]	~70% improvement in wear resistance against untreated SS. Stress corrosion cracking is also minimized
Cobalt alloys	Stress shielding, biocompatibility, toxicity	Carburizing[84]	Corrosion resistance enhanced due to passive film S-phase
		Ion implantation with O_2 and N_2 atoms[83]	Stable passive layer Cr_2O_3. Corrosion rate minimizes the toxicity
Titanium alloys	Poor wear resistance	Carburizing[59]	Hard TiC layer formation
		Plasma nitriding[56]	TiN multilayer can be productive to combat wear
Magnesium alloys	Corrosion	Electrodeposited HAP layers on Mg–Zn alloy[44]	Better corrosion resistance but delay in bone formation
		FSP with reinforcements HAP[94]	

nitrogen makes the alloy brittle, which is a concern. Hence, there is a dire need for biocompatibility through low-cost diffusion-based processes. In today's scenario, hybrid or duplex coatings can cater to the demands of many implants.

CoCrMo alloys in the wrought form are preferred in joint replacement, particularly at load-bearing sites. However, their high cost limits their commercial viability.

For Ti alloys, there exists a vast scope to improve their wear resistance. Ion implantation seems to work effectively for these alloys to address the problems mentioned above. Although surface modifications suggest corrosion resistance for these implants, the studies concerning metal ion release and cell proliferation are scanty. This information is needed to obtain a better insight into the biocompatibility of these implants.

Mg alloys have led to the genesis of a new class of degradable biomaterials and are gaining interest in orthopedics and tissue engineering. These tend to less toxic and can be tolerated by the human body even at relatively high concentrations. One of the major concerns is the evolution of hydrogen. Efforts are made to alleviate this problem. Similarly, metallic glasses of bioinert material like Ti and bioresorbable materials like Fe and Zn offer a good combination of elastic modulus, elastic strains and strength.

Further, appropriate surface characteristics can control wear and corrosion; these qualities with bioresorbability make such metallic materials a potent option for bone screws, plates, and interlocking nails. Nonetheless, due to their amorphous nature, a detailed study of crack propagation occurring during physiological conditions would instil

confidence in biological class bulk metallic glasses. Therefore, the implant design has to consider biomechanical features to make the implants more workable. FSP has been offering significant benefits for in vivo applications.

As far as lower-temperature surface modification of Mg and its alloys is concerned, electrodeposition of HA and chemical etching are the most promising and straightforward techniques to control degradation by corrosion. In the former case, the process can ameliorate cytocompatibility, while, in the latter case, the surface can react to produce a passive stable layer of $Mg(OH)_2$ to control the corrosion rate.

The faster degradation of implants invites routine surgery, which is marred by hemolysis and osteolysis. So, to curb such issues, firstly, the alloys could be sintered by advanced techniques, such as hot pressing, spark plasma sintering, and microwave sintering, to refine the grain stricture and reduce porosity. Secondly, the FSP of these implants can produce a homogenous microstructure with finer grain size. Also, alloying elements ameliorate the strength and biocompatibility. Sophisticated vapor deposition techniques could be combined with conventional coatings to achieve multi-layered coatings thus improving the longevity of biocompatible orthopedic implants.

For successful clinical trials, biomechanical research data of the designed and the developed implants are essential to evaluate the bone-implant interfacial strength and other biomechanical properties. Thus, Mg and its alloy's degradation rate can be controlled and can be an indispensable alternative among orthopedic implants.

CONCLUSIONS

Although traditional metallic implants suffer from drawbacks, they remain a preferred choice for orthopedic applications as their microstructure can be tailored to obtain superior mechanical properties. However, their service life has been a significant concern.

Biodegradable implants embrace market caps; the areas to focus on are bio-corrosion and their excretion mechanism and exploration of new alloys. Interestingly, diffusion-based low-temperature surface techniques are gathering consensus owing to their unique capabilities.

The diffusion-based low-temperature surface modifications offer the following advantages:

(a) The coating thickness ranges from a few nm to μm.
(b) Economical, reliable and high-quality coatings.
(c) An increase in hardness, wear resistance, improved corrosion resistance.
(d) Biocompatibility with sound osseointegration and cell growth.

The friction-stir process offers the following advantages:

i. Homogeneity in microstructure and grain refinement could improve mechanical properties.
ii. Appropriate alloying elements can hinder the hydrogen evolution rate that limits the pitting corrosion.
iii. Biocompatibility with osseointegration leads to cell growth and proliferation.

In conclusion, diffusion-based, low-temperature surface modification techniques have gained attention due to their outstanding performance in the development of orthopedic implants to meet future challenges. Also, hybrid coating techniques, such as vapor deposition amalgamated with conventional surface modification techniques cannot be ruled out from the current scenario.

ACKNOWLEDGEMENT

CONFLICT OF INTEREST

On behalf of all authors, the corresponding author states that there is no conflict of interest.

REFERENCES

1. G. Song, *Corros. Sci.* 49, 1696. (2007).
2. T.S. Sudarshan, T.S. Srivatsan, and D.P. Harvey, *Eng. Fract. Mech.* 36, 827. (1990).
3. H. Amel-Farzad, M.T. Peivandi, and S.M.R. Yusof-Sani, *Eng. Fail. Anal.* 14, 1205. (2007).
4. M. Manrique-Moreno, F. Villena, C.P. Sotomayor, A.M. Edwards, M.A. Munoz, P. Garidel, and M. Suwalsky, *Biochim. Biophys. Acta* 1808, 2656. (2011).
5. M. Niinomi, M. Nakai, and J. Hieda, *Acta Biomater.* 8, 3888. (2012).
6. A. Balamurugan, S. Rajeswari, G. Balossier, A.H.S. Rebelo, and J.M.F. Ferreira, *Mater. Corros.* 59, 855. (2008).
7. S. Zlotnik, M. Maltez-da Costa, N. Barroca, M.J. Hortigüela, M.K. Singh, M.H.V. Fernandes, and P.M. Vilarinho, *J. Mater. Chem. B* 7, 2177–2189. (2019).
8. T. Roland, D. Retraint, K. Lu, and J. Lu, *Scr. Mater.* 54, 1949. (2006).
9. M. Taira, and E.P. Lautenschlager, *J. Biomed. Mater. Res.* 26, 1131. (1992).
10. L.M. Weldon, P.E. McHugh, W. Carroll, E. Costello, and C. O'Bradaigh, *J. Mater. Sci. Mater. Med.* 16, 107. (2005).
11. A. Ralls, P. Kumar, M. Misra, and P.L. Menezes, *JOM* 72, 684. (2019).
12. M. Kaur, and K. Singh, *Mater. Sci. Eng. C* 102, 844. (2019).
13. M. Niinomi, *Sci. Technol. Adv. Mater.* 4, 445. (2016).
14. L.C. Zhang, and L.Y. Chen, *Adv. Eng. Mater.* 21, 1801215. (2019).
15. S. Yaghoubi, C.W. Schwietert, and J.P. McCue, *Biol. Trace Elem. Res.* 78(1), 205. (2000).
16. M. Geetha, A.K. Singh, R. Asokamani, and A.K. Gogia, *Prog. Mater Sci.* 54, 397. (2009).
17. M. Niinomi, *Mater. Trans.* 49, 2170. (2008).
18. D. Raducanu, V.D. Cojocaru, A. Nocivin, I. Cinca, N. Serban, and E.M. Cojocaru, *JOM* 72, 2937. (2020).

19. M.S.K.K.Y. Nartu, D. Flannery, S. Mazumder, S.A. Mantri, S.S. Joshi, A.V. Ayyagari, B. McWilliams, K. Cho, N.B. Dahotre, and R. Banerjee, *JOM* 73, 1819. (2021).

20. D.J. Paustenbach, D.A. Galbraith, and B.L. Finley, *Clin. Toxicol. (Phila)* 52, 98. (2014).

21. J. Alvarado, R. Maldonado, J. Marxuach, and R. Otero, *Eng. Appl. Mech. Med.* 4, 6. (2003).

22. J. Nagels, M. Stokdijk, and P.M. Rozing, *J. Shoulder Elbow Surg.* 12, 35. (2003).

23. Z. Qiao, Z. Shi, N. Hort, N.I.Z. Abidin, and A. Atrens, *Corros. Sci.* 61, 185–207. (2012).

24. H.E. Friedrich, and B.L. Mordike, *Magnesium Technology*, 1st edn. (Springer, New York, 2006), p 677.

25. Y.F. Zheng, X.N. Gu, and F. Witte, *Mater. Sci. Eng. R* 77, 1. (2014).

26. Z. Pu, G.L. Song, S. Yang, J.C. Outeiro, O.W. Dillon, D.A. Puleo, and I.S. Jawahir, *Corros. Sci.* 57, 192. (2012).

27. I. Etim, W. Zhang, T. Liu, H. Zhao, L. Tan, and K. Yang, *JOM* 73, 1754. (2021).

28. H. Hermawan, D. Dube, and D. Mantovani, *J. Biomed. Mater. Res. A* 93, 1. (2010).

29. M. Moravej, and D. Mantovani, *Int. J. Mol. Sci.* 12, 4250. (2011).

30. M. Schinhammer, A.C. Hanzi, J.F. Loffler, and P.J. Uggowitzer, *Acta Biomater.* 6, 1705. (2010).

31. H. Hermawan, H. Alamdari, D. Mantovani, and D. Dubé, *Powder Metall.* 51, 38. (2013).

32. H. Hermawan, D. Dubé, and D. Mantovani, *Adv. Mater. Res.* 15–17, 107. (2006).

33. V.R. Malik, P.A. Bajakke, S.C. Jambagi, C. Nagarjuna, and A.S. Deshpande, *JOM* 72, 3582. (2020).

34. J. Lin, Y. Wang, D. Sun, H. Xue, R.-G. Guan, and H. Liu, *JOM* 72, 3661. (2020).

35. K. Prasad, O. Bazaka, M. Chua, M. Rochford, L. Fedrick, J. Spoor, R. Symes, M. Tieppo, C. Collins, A. Cao, D. Markwell, K.K. Ostrikov, and K. Bazaka, *Materials* 10, 884. (2017).

36. A. Bekmurzayeva, W.J. Duncanson, H.S. Azevedo, and D. Kanayeva, *Mater. Sci. Eng. C* 93, 1073. (2018).

37. T. Hryniewicz, *Surf. Coat. Technol.* 64, 75. (1994).

38. A. Latifi, M. Imani, M.T. Khorasani, and M.D. Joupari, *Surf. Coat. Technol.* 221, 1. (2013).

39. A.A. John, S.K. Jaganathan, E. Supriyanto, and A. Manikandan, *Curr. Sci.* 111, 1003. (2016).

40. V.K. Balla, M. Das, S. Bose, G.D. Ram, and I. Manna, *Mater. Sci. Eng. C* 33, 4594. (2013).

41. H. Mas Ayu, R. Daud, T. Kurniawan, J. Alias, S. Izman, A. Shah, and M. Anwar, *Materwiss. Werksttech* 50, 254. (2019).

42. R. Bosco, J. Van Den Beucken, S. Leeuwenburgh, and J. Jansen, *Coatings* 2, 95. (2012).

43. V. Huynh, N.K. Ngo, and T.D. Golden, *Int. J. Biomater.* 2019, 1. (2019).

44. P. Chakraborty Banerjee, S. Al-Saadi, L. Choudhary, S.E. Harandi, and R. Singh, *Materials* 12, 136. (2019).

45. S. Cometa, M.A. Bonifacio, M. Mattioli-Belmonte, L. Sabbatini, and E. De Giglio, *Coatings* 9, 268. (2019).

46. Y. Sasikumar, K. Indira, and N. Rajendran, *J. Bio-Tribo-Corros.* 5, 1. (2019).

47. L. Thijs, F. Verhaeghe, T. Craeghs, J.V. Humbeeck, and J.-P. Kruth, *Acta Mater.* 58, 3303. (2010).

48. A. Chateauminois, *Tribol. Int* 33, 67. (2000).

49. P.A. Bajakke, S.C. Jambagi, V.R. Malik, and A.S. Deshpande, in *Friction Stir Processing: An Emerging Surface Engineering Technique*. ed. by K. Gupta (Springer, New York, 2020), p. 31.

50. D.K. Dwivedi, in *Surface Engineering*. ed. by D.K. Dwivedi (Springer, New Delhi, 2018), p. 16.

51. S.C. Jambagi, *Property Improvement of Thermally Sprayed Coatings Using Carbon Nanotube Reinforcement* [Dissertation], IIT, Kharagpur, Kharagpur (2017).

52. A. Dehghanghadikolaei, and B. Fotovvati, *Materials* 12, 1795. (2019).

53. S.C. Jambagi, and P.P. Bandyopadhyay, *J. Mater. Eng. Perform.* 28, 7347. (2019).

54. A. Goharian, and M.R. Abdullah, in *Bioinert Metals (Stainless Steel, Titanium, Cobalt Chromium)*. ed. by A. Goharian (Elsevier, Amsterdam, 2017), p. 115.

55. S. Izman, M. Rafiq, M. Anwar, E.M. Nazim, R. Rosliza, A. Shah, and M.A. Hass, in *Surface Modification Techniques for Biomedical Grade of Titanium Alloys: Oxidation, Carburization and Ion Implantation Processes*. ed. by A.K.M.N. Amin (InTech, Croatia, 2012), p. 228.

56. A. Samanta, R. Rane, B. Kundu, D. Kr. Chanda, J. Ghosh, S. Bysakh, G. Jhala, A. Joseph, S. Mukherjee, M. Das, and A.K. Mukhopadhyay, *Appl. Surf. Sci.* 507, 145009. (2020).

57. S. Sobieszczyk, *Adv. Mater. Sci.* 10, 29. (2010).

58. K. Bordjih, J.-Y. Jouzeau, D. Mainard, E. Payan, J.-P. Delagoutte, and P. Netter, *Biomaterials* 17, 491. (1996).

59. Y. Luo, X. Rao, T. Yang, and J. Zhu, *J. Tribol.* 140, 031604–031611. (2018).

60. F. Czerwinski, in *Thermochemical Treatment of Metals*. ed. by F. Czerwinski (Intech, Croatia, 2012), p. 73.

61. I. Özbek, B.A. Konduk, C. Bindal, and A.H. Ucisik, *Vacuum* 65, 521. (2002).

62. M. Uddin, C. Hall, and V. Santos, *Surf. Coat. Technol.* 385, 125363. (2020).

63. N.N.C. Isa, Y. Mohd, and N. Yury, Effect of chitosan on the formation of hydroxyapatite (HAp) coatings on titanium by electrodeposition technique, in, *Proceedings of the IEEE colloquium on humanities, science and engineering*, Kota Kinabalu, Malaysia, p. 776 (2012).

64. R.B. Durairaj, *Int. J. Electrochem. Sci* 13, 4841. (2018).

65. T.N. Pham, T.M. Thanh Dinh, T.T. Nguyen, T.P. Nguyen, E. Kergourlay, D. Grossin, G. Bertrand, N. Pebere, S.J. Marcelin, C. Charvillat, and C. Drouet, *Adv. Nat. Sci. Nanosci. Nanotechnol.* 8, 035001. (2017).

66. P. Ducheyne, W. Van Raemdonck, J.C. Heughebaert, and M. Heughebaert, *Biomaterials* 7, 97. (1986).

67. G.A. Afolaranmi, J. Tettey, R.M. Meek, and M.H. Grant, *Open Orthop. J.* 2, 10. (2008).

68. L. Xu, E. Zhang, and K. Yang, *J. Mater. Sci. Mater. Med.* 20, 859. (2009).

69. E. Zhang, in *Phosphate Treatment of Magnesium Alloy Implants for Biomedical Applications*. ed. by T.S.N.S. Narayanan, I.-S. Park, and M.-H. Le (Woodhead, Cambridge, 2015), p. 57.

70. T.R. Rautray, R. Narayanan, and K.-H. Kim, *Prog. Mater Sci.* 56, 1137. (2011).

71. Z.A. Uwais, M.A. Hussein, M.A. Samad, and N. Al-Aqeeli, *Arab. J. Sci. Eng.* 42, 4493. (2017).

72. U. Kamachimudali, T.M. Sridhar, and B. Raj, *Sadhana* 28, 601. (2003).

73. A.Y.C. Nee, *Handbook of Manufacturing Engineering and Technology*, 1st edn. (Springer, New York, 2015), p 3500.

74. R.S. Mishra, and Z.Y. Ma, *Mater. Sci. Eng. R* 50, 1. (2005).

75. V. Malik, and S.V. Kailas, *J. Mater. Process. Technol.* 258, 80. (2018).

76. V. Malik, and S.V. Kailas, *Proc. Inst. Mech. Eng. C J. Mech. Eng. Sci.* 235, 744. (2020).

77. P.A. Bajakke, V.R. Malik, and A.S. Deshpande, *Mater. Manuf. Processes* 34, 833. (2019).

78. V. Malik, N.K. Sanjeev, and P. Bajakke, *Int. J. Manuf. Res* 15, 107. (2020).

79. W. Suchanek, and M. Yoshimura, *J. Mater. Res.* 13, 94. (2011).

80. D.T. Thanh, P.T. Nam, N.T. Phuong, X. Que le, N.V. Anh, T. Hoang, and T.D. Lam, *Mater. Sci. Eng. C* 33, 2037. (2013).

81. R. Davalos Monteiro, J. van de Wetering, B. Krawczyk, and D.L. Engelberg, *Met. Mater. Int.* 26(5), 630–640. (2020).

82. A.S. Hammood, M.S. Naser, and Z.S. Radeef, *JOM* 73, 524. (2020).

83. C. Diaz, J.A. Garcia, S. Mandl, and R.J. Rodriguez, *IEEE Trans. Plasma Sci* 39, 3045. (2011).

84. J. Cassar, B. Mallia, A. Karl, and J. Buhagiar, *Surf. Coat. Technol.* 292, 90. (2016).

85. E. Czarnowska, T. Wierzchoń, and A. Maranda-Niedbała, *J. Mater. Process. Technol.* 92–93, 190. (1999).
86. G.H. Zhang, P.Z. Zhang, M.Z. Yu, and Z. Xu, *Adv. Mater. Res.* 47–50, 1197. (2008).
87. S. Virtanen, *Mater. Sci. Eng. B* 176, 1600. (2011).
88. S. Agarwal, J. Curtin, B. Duffy, and S. Jaiswal, *Mater. Sci. Eng. C* 68, 948. (2016).
89. G.P.S. Sodhi, and H. Singh, *IOP Conf. Ser. Mater. Sci. Eng.* 284, 012026. (2018).
90. Y. Song, S. Zhang, J. Li, C. Zhao, and X. Zhang, *Acta Biomater.* 6, 1736. (2010).
91. J. Chen, L. Tan, X. Yu, I.P. Etim, M. Ibrahim, and K. Yang, *J. Mech. Behav. Biomed. Mater.* 87, 68. (2018).
92. M.B. Kannan, W. Dietzel, and R. Zettler, *J. Mater. Sci. Mater. Med.* 22, 2397. (2011).
93. C. Liu, Z. Ren, Y. Xu, S. Pang, X. Zhao, and Y. Zhao, *Scanning* 2018, 1. (2018).
94. B. Ratna Sunil, T.S. Sampath Kumar, and C. Uday, *Mater. Sci. Forum* 710, 264. (2012).
95. M. Abbasi, B. Bagheri, M. Dadaei, H.R. Omidvar, and M. Rezaei, *J. Adv. Manuf. Technol.* 77, 2051. (2014).
96. Y. Mazaheri, M.M. Jalilvand, A. Heidarpour, and A.R. Jahani, *Tribol. Int* 143, 106062. (2020).
97. G.H. Zhao, R.E. Aune, and N. Espallargas, *J. Mech. Behav. Biomed. Mater.* 63, 100. (2016).
98. P. Asadi, M.K.B. Givi, N. Parvin, A. Araei, M. Taherishargh, and S. Tutunchilar, *J. Adv. Manuf. Technol.* 63, 987. (2012).

99. G. Madhusudhan Reddy, A. Sambasiva Rao, and K. Srinivasa Rao, *Trans. Indian Inst. Met.* 66, 13. (2012).
100. K. Kudła, J. Iwaszko, K. Fila, and M. Strzelecka, *Arch. Metall. Mater.* 61, 1555. (2016).
101. D. Liu, R. Xin, L. Zhao, Y. Hu, and J. Zhang, *Sci. Technol. Weld. Join* 22, 601. (2017).
102. M. Vignesh Kumar, G. Padmanaban, and V. Balasubramanian, *Materwiss. Werksttech.* 51, 140. (2020).
103. S.C. Jambagi, *J. Alloys Compd.* 728, 126. (2017).
104. S.C. Jambagi, A. Agarwal, N. Sarkar, and P.P. Bandyopadhyay, *J. Mater. Eng. Perform.* 27, 2364. (2018).
105. J.E. Tercero, S. Namin, D. Lahiri, K. Balani, N. Tsoukias, and A. Agarwal, *Mater. Sci. Eng. C* 29, 2195. (2009).
106. V. Kain, in *Stress Corrosion Cracking (SCC) in Stainless Steels*. ed. by V.S. Raja, and T. Shoji (Woodhead, Cambridge, 2011), p. 199.
107. U.S.F.D. Administration, *Safety of Metals and Other Materials Used in Medical Devices* "(FDA, 2021), https://www.fda.gov/medical-devices/products-and-medical-procedures/safety-metals-and-other-materials-used-medical-devices. Accessed 20 July 2021.